



## RESEARCH ARTICLE

# Deletion of Tgf $\beta$ signal in activated microglia prolongs hypoxia-induced retinal neovascularization enhancing Igf1 expression and retinal leukostasis

Ayumi Usui-Ouchi<sup>1,2</sup>  | Kevin Eade<sup>1,3</sup> | Sarah Giles<sup>3</sup> | Yoichiro Ideguchi<sup>1</sup> | Yasuo Ouchi<sup>4,5</sup> | Edith Aguilar<sup>1</sup> | Guoqin Wei<sup>1</sup> | Kyle V. Marra<sup>1,6</sup> | Rebecca B. Berlow<sup>7</sup> | Martin Friedlander<sup>1,3</sup> 

<sup>1</sup>Department of Molecular Medicine, The Scripps Research Institute, La Jolla, California, USA

<sup>2</sup>Department of Ophthalmology, Juntendo University Urayasu Hospital, Chiba, Japan

<sup>3</sup>The Lowy Medical Research Institute, La Jolla, California, USA

<sup>4</sup>Gene Expression Laboratory, Salk Institute for Biological Studies, La Jolla, California, USA

<sup>5</sup>Department of Regenerative Medicine, Chiba University Graduate School of Medicine, Chiba, Japan

<sup>6</sup>Department of Bioengineering, University of California San Diego, La Jolla, California, USA

<sup>7</sup>Department of Integrative Structural and Computational Biology, The Scripps Research Institute, La Jolla, California, USA

## Correspondence

Martin Friedlander, Department of Molecular Medicine, The Scripps Research Institute, 10550 North Torrey Pines Road, La Jolla, CA 92037, USA.

Email: [friedlan@scripps.edu](mailto:friedlan@scripps.edu)

## Funding information

Japan Society for the Promotion of Science, Grant/Award Numbers: 17K16984, 21K09727; Lowy Medical Research Institute; National Eye Institute, Grant/Award Number: EY11254; Suzuki Manpei Diabetes Foundation

## Abstract

Retinal neovascularization (NV) is the major cause of severe visual impairment in patients with ischemic eye diseases. While it is known that retinal microglia contribute to both physiological and pathological angiogenesis, the molecular mechanisms by which these glia regulate pathological NV have not been fully elucidated. In this study, we utilized a retinal microglia-specific Transforming Growth Factor- $\beta$  (Tgf $\beta$ ) receptor knock out mouse model and human iPSC-derived microglia to examine the role of Tgf $\beta$  signaling in activated microglia during retinal NV. Using a tamoxifen-inducible, microglia-specific Tgf $\beta$  receptor type 2 (Tgf $\beta$ r2) knockout mouse [Tgf $\beta$ r2 KO ( $\Delta$ MG)] we show that Tgf $\beta$  signaling in microglia actively represses leukostasis in retinal vessels. Furthermore, we show that Tgf $\beta$  signaling represses expression of the pro-angiogenic factor, Insulin-like growth factor 1 (Igf1), independent of Vegf regulation. Using the mouse model of oxygen-induced retinopathy (OIR) we show that Tgf $\beta$  signaling in activated microglia plays a role in hypoxia-induced NV where a loss in Tgf $\beta$  signaling microglia exacerbates and prolongs retinal NV in OIR. Using human iPSC-derived microglia cells in an in vitro assay, we validate the role of Transforming Growth Factor- $\beta$ 1 (Tgf $\beta$ 1) in regulating Igf1 expression in hypoxic conditions. Finally, we show that Tgf $\beta$  signaling in microglia is essential for microglial homeostasis and that the disruption of Tgf $\beta$  signaling in microglia exacerbates retinal NV in OIR by promoting leukostasis and Igf1 expression.

## KEYWORDS

a mouse model of oxygen-induced retinopathy, angiogenesis, diabetic retinopathy, hypoxia, insulin like growth factor 1, ischemic retinopathy, microglia, neovascularization, retinopathy of prematurity, transforming growth factor

## 1 | INTRODUCTION

Retinal neovascularization (NV) is the major cause of severe visual impairment in patients with ischemic or inflammatory ocular diseases

such as diabetic retinopathy, retinal vein occlusion, uveitis and retinopathy of prematurity (Usui et al., 2015). Vascular Endothelial Growth Factor (VEGF) plays a pivotal role in the development of pathological NV; drugs that inhibit this pro-angiogenic cytokine have been

This is an open access article under the terms of the [Creative Commons Attribution](https://creativecommons.org/licenses/by/4.0/) License, which permits use, distribution and reproduction in any medium, provided the original work is properly cited.

© 2022 The Authors. GLIA published by Wiley Periodicals LLC.

widely used to treat retinal neovascular diseases (Fogli et al., 2018; Witmer et al., 2003). While intravitreal anti-VEGF injection represents a major breakthrough for the treatment of retinal neovascular diseases, not all patients respond to anti-VEGF agents (Ashraf et al., 2016; Ip et al., 2015; Writing Committee for the Diabetic Retinopathy Clinical Research et al., 2015). Moreover, there are safety issues associated with repeated intravitreal administration of anti-VEGF agents, especially for at-risk patients with diabetes, cardio- and cerebrovascular diseases, or premature babies who are vulnerable to modulation of crucial trophic factors (Falavarjani & Nguyen, 2013; Usui-Ouchi & Friedlander, 2019). Understanding VEGF-independent mechanisms of retinal NV and their role in retinal neovascular disease is critical for developing additional complimentary or alternative therapeutic strategies.

Numerous studies have shown that dysregulation of the VEGF-independent pro-angiogenic factor Insulin Growth Factor 1 (Igf1) is associated with pathological NV in proliferative diabetic retinopathy or retinopathy of prematurity (Boulton et al., 1997; Haurigot et al., 2009; Hellstrom et al., 2001; Kondo et al., 2003; Meyer-Schwickerath et al., 1993; Ruberte et al., 2004; Smith et al., 1999; Wilkinson-Berka et al., 2006). In patients with proliferative diabetic retinopathy, vitreous levels of IGF1 are increased (Boulton et al., 1997; Grant et al., 1986; Meyer-Schwickerath et al., 1993). In mouse OIR models, endothelial cell specific IGF1 receptor KO mice show reduced retinal NV (Kondo et al., 2003), and overexpression of IGF1 in the retina results in phenotypic changes similar to those of diabetic retinopathy (pericyte loss, capillary basement membrane thickness, inner retinal microaneurysms, and neovessels) (Ruberte et al., 2004). IGF1 plays a key role in pathological NV in retina, however the origin and regulation of IGF1 has not been fully characterized.

Microglia are the resident immune cells in the retina localized to the outer and inner plexiform layers and superficial plexus, engaging in surveillance and maintenance of retinal synapses (Lee et al., 2008; Wang et al., 2016). Under pathological conditions such as retinal degeneration, neovascularization and aging, microglia are activated and migrate into the affected sites where they respond to inflammation by up-regulating phagocytic activity and expression of inflammatory cytokines (Ma et al., 2009; Usui-Ouchi et al., 2020; Zhao et al., 2015). Activated and mis-localized retinal microglia are a common hallmark of various retinal degenerative, inflammatory and angiogenic diseases (Silverman & Wong, 2018). In ischemic retinopathy, activated microglia are found in the central avascular zone prior to neovascularization (Fischer et al., 2011; Vessey et al., 2011). In the OIR mouse model of ischemic retinopathy, ablation of microglia can rescue NV (Kubota et al., 2009) suggesting a key role in pathological NV. However, their role appears to be independent of VEGF activation (Boeck et al., 2020). The mechanism by which microglia are activated and promote NV is not understood.

Tgfb1 has previously been shown to be a potent immunoregulatory factor for microglia in vivo and in vitro where the loss of Tgfb signaling results in the increase of microglia activation (Brionne et al., 2003; Butovsky et al., 2014; Ma et al., 2019; Spittau

et al., 2013; Zoller et al., 2018). Tgfb signaling is propagated by binding of Tgfb to Tgfb receptor type 2 (Trfb2) that phosphorylates the Tgfb receptor type 1 (Tgfb1) (Wrana et al., 1994; Yamashita et al., 1994). Pan-ocular deletion of Tgfb signaling can also cause common changes observed in proliferative diabetic retinopathy including pericyte loss, microaneurysms, leaky capillaries, and retinal hemorrhages (Braunger et al., 2015). Targeted ablation of Tgfb2 in retinal microglia promotes activation causing a neuroinflammatory response and choroidal NV (W. Ma et al., 2019). However, the role of Tgfb signaling in microglia on retinal NV and the mechanisms that regulate microglia function during ischemia are not understood.

Here, we investigate the role of Tgfb signaling in the activation of microglia and demonstrate that it can induce VEGF-independent NV pathways through regulation of Igf1. Using the OIR mouse model of ischemic retinopathy, targeted ablation of Tgfb2 in microglia, and human iPSC derived microglia we demonstrate that hypoxia in the retina regulates microglial activation, the expression of chemoattractant chemokines, leukostasis, and Igf1 dependent NV through the repression of Tgfb signaling in microglia. These results provide insight into the mechanism of microglial activation under ischemic retina and the role they play in the formation of pathological NV.

## 2 | MATERIALS AND METHODS

### 2.1 | Mice and animal experimental procedures

All animal protocols were approved by the IACUC committee at The Scripps Research Institute, La Jolla, California. All animals received food and water ad libitum. C57BL6 mice and Balb/c mice were obtained from The Scripps Research Institute animal facility. Chemokine (C-X3-C motif) receptor 1 (Cx3cr1)<sup>Cre-ERT</sup> mice expressing tamoxifen-inducible Cre recombinase (The Jackson Laboratory, #021160) (Parkhurst et al., 2013) were crossed with mice possessing loxP sites that flank exon 4 of the Tgfb2 (Tgfb2<sup>flox/flox</sup>, The Jackson Laboratory, #012603) (Leveen et al., 2002) to generate Cx3cr1<sup>Cre-ERT</sup>; Tgfb2<sup>flox/flox</sup>. To induce Cx3cr1-Cre recombination, 100 µg of tamoxifen (Sigma-Aldrich, T5648)/cone oil solution was administered to Cx3cr1<sup>Cre-ERT</sup>; Tgfb2<sup>flox/flox</sup> and control littermates, Tgfb2<sup>flox/flox</sup> (Control) subcutaneously once a day from P9 to P14 and for OIR P4 to P6 and P12 to P14 to avoid the oxygen level fluctuation in chamber from P7 to P12. Oxygen-induced retinopathy (OIR) was induced as previously described (Murinello et al., 2019; Smith et al., 1994). Postnatal day 7 (P7) pups and their mothers were exposed to 75% oxygen in a hyperoxia chamber (BioSpherix ProOx P110) for 5 days and returned to room air at P12. Mice were euthanized by cervical dislocation at varying time points, as indicated in the results and figure legends.

### 2.2 | Cell and cell culture

The human induced pluripotent stem cell (hiPSC) line used was derived from peripheral blood mononuclear cells from a female.

Reprogramming was performed by the Harvard iPS core facility using sendai virus for reprogramming factor delivery. All cell lines were obtained with verified normal karyotype and contamination-free. hiPSC were maintained on Matrigel (BD Biosciences) coated plates with mTeSR1 medium (STEMCELL Technologies). Cells were passaged every 3–4 days at approximately 80% confluence. Colonies containing clearly visible differentiated cells were marked and mechanically removed before passaging. Microglia precursors were generated as previously described (Haenseler et al., 2017; van Wilgenburg et al., 2013). The embryoid bodies (EBs) are formed using Aggrewells (STEMCELL Technologies), cultured with bone morphogenetic protein 4 (BMP4), vascular endothelial growth factor (VEGF), and stem cell factor (SCF), then plated into T175 flasks with Interleukin-3 and macrophage colony-stimulating factor (M-CSF). After 4 weeks, microglia precursors emerged into the supernatant. It was previously revealed that their ontogeny is MYB-independent primitive myeloid cells, which is same ontogeny as microglia (Buchrieser et al., 2017). hiPS derived Microglia precursors (pMG) were plated into 12 well plates containing X-VIVO15 with 100 ng/ml M-CSF, 2 mM Glutamax, 100 U/ml penicillin, and 100 µg/ml streptomycin for further in vitro assays. The cells were stimulated with human recombinant Tgfb1 (Peprotech, 100-21), 10 µM of SB525334 (Selleckchem, S1476), 200 µM of DMOG (Millipore sigma, D3695), then cell culture supernatant and cells were stored at –80°C for following qPCR and ELISA assays.

### 2.3 | Immunohistochemistry of whole-mount retinas

Enucleated eyes were placed in 4% paraformaldehyde (PFA) for 1 h. After fixation, the cornea, the lenses, the sclera, choroid, and the vitreous were removed and the retinas were laid flat with four radial relaxing incisions. Retinas were incubated in blocking buffer (PBS with 10% fetal bovine serum, 10% normal goat serum, and 0.2% Triton X-100) for 2 h at 4°C, following by an overnight incubation with primary antibodies in blocking buffer at 4°C. Tissue specimens were then washed and incubated with the corresponding Alexa fluorescent-conjugated secondary antibodies (Thermo Fisher) for 3 h. Retinas were washed in PBS and mounted with ProLong Diamond Antifade mounting medium (Thermo Fisher Scientific, P36965). Primary antibodies targeting IBA1 (1:500; FUJIFILM, 019-19741), and NG2 (1:200; Millipore, AB5320) were used. Fluorescent-conjugated isolectin Griffonia simplicifolia IB-4 (GS-lectin) (1:200; Thermo Fisher Scientific, I21413, I32450) was also used for labeling endothelial cells. For detecting hypoxic cells in vivo, 60 mg/kg bodyweight pimonidazole hydrochloride (Hypoxyprobe-1™ kit, hpi), diluted in PBS was administered by intraperitoneal injection 1 h prior to euthanasia. Enucleated eyes were processed as above and stained with FITC anti-pimonidazole antibody (1:100, Hypoxyprobe-1™ kit, hpi). All images were acquired with a confocal laser scanning microscope (LSM 710, Zeiss) and processed with the ZEN 2010 software (Zeiss).

### 2.4 | Retinal microglia isolation by flow cytometry

A postnatal neural dissociation kit (Miltenyi, 130-092-628) was used to prepare a single cell suspension from mouse retinas. Cells were centrifuged at 150g for 5 min at 4°C. The digested tissue was resuspended in 100 µl of 4% FBS in PBS containing an FITC antibody to CD11b (1:100; BioLegend, 101206) and PE antibody to Gr-1 (1:100; BD Biosciences, 553128) and incubated for 20 min on ice. The cells were washed and suspended with 1 ml of 4% FBS/PBS containing DAPI (1:2000; Thermo Fisher Scientific, 62248) and DRAQ5 (1:5000; Cell signaling, 40845) for exclusion of dead cells and debris. We used clone RB6-8C5 for Gr-1 antibody because it reacts with a common epitope on Ly6-G and Ly6-C to eliminate blood born monocytes and granulocytes. We did not use CD45 antibody to detect CD45<sup>low</sup> fraction as microglia population because CD45 expression in Tgfb2-ablated microglia is upregulated transforming to activated form as previously shown (Ma et al., 2019). Labeled retinal microglia (CD11b positive and Gr-1 negative in DAPI negative and DRAQ5 positive cells) were isolated by fluorescence-activated cell sorting (FACS) (MoFlo Astrios EQ; Beckman Coulter) at the Scripps Flow Cytometry Core Facility. Sorted cells were resuspend in 350ul of RLT buffer from RNeasy Micro Kit (QIAGEN) and stored at –80°C.

### 2.5 | RNA isolation and real-time PCR

For whole retina and culture cells, single retinas were collected in 500 µl of Trizol and total RNA was isolated using a PureLink RNA Mini Kit (Thermo Fisher Scientific) according to manufacturer's instructions. Seven hundred and fifty nanograms of RNA was used for RT-qPCR using a high-capacity cDNA reverse transcription kit (Thermo Fisher Scientific). For flow-sorted cells, total RNA was isolated from sorted cells using the RNeasy Micro Kit (QIAGEN) and reverse transcribed using Maxima First Strand cDNA Synthesis Kit for RT-qPCR (Thermo Scientific). qPCR was performed using Power-up SYBR™ Green PCR Master Mix (Thermo Fisher Scientific) and primers on a Quantstudio 5 Real-Time PCR System (Thermo Fisher Scientific).  $\beta$ -actin (*Actb*) was used as the reference gene for all experiments. Levels of mRNA expression were normalized to those in controls as determined using the comparative CT ( $\Delta\Delta CT$ ) method. Primer sequences are listed in Table S1.

### 2.6 | Enzyme-linked immunosorbent assay (ELISA)

Forty-eight hours after Tgfb1 supplementation to hiPS derived pMG, cell culture supernatants were assayed for ELISA assay to detect the protein level of IGF1 using the Human IGF-1 Quantikine ELISA kit (R&D systems) according to the manufacturer's protocol.

### 2.7 | Lectin labelling of adherent retinal leukocytes

The retinal vasculature and adherent leukocytes were imaged by perfusion labeling with TRITC-conjugated Concanavalin A (Con A) lectin

(Vector Laboratories), as described previously (Joussen et al., 2001; Okunuki et al., 2019). Briefly, after deep anesthesia, the chest cavity was opened and a 27-gauge cannula was inserted into the left ventricle. Mice were then perfused through the left ventricle first using 5 ml of PBS, followed by fixation with 1% PFA (5 ml), 5 ml of TRITC-conjugated Con A (20  $\mu$ g/ml in PBS), and 5 ml of PBS. The eyes were then fixed in 4% PFA for an hour, and the retinas were flat-mounted. The total number of TRITC positive adherent leukocytes in the retinal vessels was counted.

## 2.8 | Quantification and statistical analysis

For OIR, the percentage of the area of NV and vaso-obliteration (VO) in OIR retinas was automatically quantified using deep learning segmentation software available at <http://oirseg.org> (Xiao et al., 2017). All statistical tests were performed in GraphPad Prism v8 (GraphPad Software, Inc). Data comparisons between two groups were performed using unpaired two-tailed Student *t*-tests. Data comparisons between multiple groups were performed with one-way ANOVA with Tukey's correction. Statistical tests used for each experiment are specified in the figure legends. Data are represented as mean  $\pm$  SEM. A *p* value of *p* < .05 was considered significant.

## 2.9 | Study approval

All animal protocols were approved by the IACUC committee at The Scripps Research Institute, La Jolla, California, and all federal animal experimentation guidelines were adhered to.

## 3 | RESULTS

### 3.1 | Tgfb $\beta$ 2 deficient microglia transform to activated status

Tgfb $\beta$ 1 has previously been shown to be a potent immunoregulatory factor for microglia *in vivo* and *in vitro* where the loss of Tgfb $\beta$  signaling results in the increase of microglia activation (Brionne et al., 2003; Butovsky et al., 2014; Ma et al., 2019; Spittau et al., 2013; Zoller et al., 2018). To investigate the role of Tgfb $\beta$  signaling in microglia activation and NV we used microglia specific Tgfb $\beta$ 2 knockout mice (Tgfb $\beta$ 2 KO ( $\Delta$ MG)) with Cx3cr1<sup>Cre-ERT</sup>; Tgfb $\beta$ 2<sup>flox/flox</sup>. As Tgfb $\beta$ 2 is highly expressed in both endothelial cells and microglia in mouse retina (Braunger et al., 2015; Ma et al., 2019), we first confirmed whether exon 4 of Tgfb $\beta$ 2 is excised specifically in microglia compared to endothelial cells in Tgfb $\beta$ 2 KO ( $\Delta$ MG) retinas 4 weeks after tamoxifen injection (Figure 1a). We performed a qPCR analysis of mRNA isolated from flow-sorted CD11b<sup>+</sup> retinal microglia and showed a marked reduction in exon 4 containing transcripts in Tgfb $\beta$ 2 KO ( $\Delta$ MG) relative to exon 3, but

not in tamoxifen-administered control mice, while the exon 4/3 ratio in CD31 positive endothelial cells was not changed in Tgfb $\beta$ 2 KO ( $\Delta$ MG) compared to control mice (Figure 1b,c). We examined microglial morphology and distribution 4 weeks after tamoxifen injection in Tgfb $\beta$ 2 KO ( $\Delta$ MG) and we found that Tgfb $\beta$ 2 deficient microglia tightly adhered to retinal vessels in all three layers: superficial plexus, intermediate plexus in the inner plexiform layer, and deep plexus in the outer plexiform layer. Tgfb $\beta$ 2 deficient microglia had shorter processes with less branching and a larger soma, while microglia from control mice did not adhere to vessels and had fine, long processes (Figure 1d,e). To examine if the activation of microglia in Tgfb $\beta$ 2 KO ( $\Delta$ MG) promotes retinal inflammation, we measured the expression of inflammatory cytokines, chemokines, and adhesion molecules in whole retina samples of Tgfb $\beta$ 2 KO ( $\Delta$ MG) and control mice by qPCR. The expression of monocyte chemoattractants Ccl2 and Ccl8 were highly upregulated, and adhesion molecules Icam1 and Vcam1 were slightly but significantly upregulated in Tgfb $\beta$ 2 KO ( $\Delta$ MG) retina compared to control retina. The expression of other proinflammatory cytokines Il6, Il1b, and Tnf and proangiogenic factors Vegfa and Igf1 were not changed in Tgfb $\beta$ 2 KO ( $\Delta$ MG) retinas (Figure 1f).

### 3.2 | Tgfb $\beta$ 2 deficient microglia promoted leukostasis via enhancing chemoattractant

To determine the consequence of the tight adherence of retinal microglia to retinal vessels in Tgfb $\beta$ 2 KO ( $\Delta$ MG), we assessed vascular development and morphology in Tgfb $\beta$ 2 KO ( $\Delta$ MG) retina 8 weeks after tamoxifen injection (Figure 2a). We first evaluated the gross morphology of retinal vessels by measuring the number of branching points and found no difference in Tgfb $\beta$ 2 KO ( $\Delta$ MG) compared to control (Figure 2b-c). Next, we evaluated the number of pericytes along retinal vasculature because pericyte loss is early pathological sign of diabetic retinopathy (Engerman, 1989). However, we found no significant difference in Tgfb $\beta$ 2 KO ( $\Delta$ MG) compared to control (Figure 2d-e). Since we found that the expression of monocyte chemoattractants Ccl2 and Ccl8 were highly upregulated and adhesion molecules Icam1 and Vcam1 were slightly but significantly upregulated in Tgfb $\beta$ 2 KO ( $\Delta$ MG) retina (Figure 1f), we next examined leukocyte recruitment and adhesion to retinal vessels. To examine the leukocyte adhesion to retinal vessels in microglia specific Tgfb $\beta$ 2 knockouts, we performed lectin labeling of adherent leukocytes. The retinal flatmount from Tgfb $\beta$ 2 KO ( $\Delta$ MG) after lectin perfusion showed adherent leukocytes in the vessels while this was not observed in the majority of control retinal flatmounts (Figure 2f-g). The adhered leukocytes expressed IBA1 suggesting that those were circulating monocytes. The number of lectin labeled adherent leukocytes was significantly higher in the retina of Tgfb $\beta$ 2 KO ( $\Delta$ MG) than in that of control (Figure 2h). Taken together, Tgfb $\beta$ 2 knock out microglia which adhered to vessels promote leukocyte adhesion via enhancing chemoattractant, without affecting retinal vascular development or morphology.

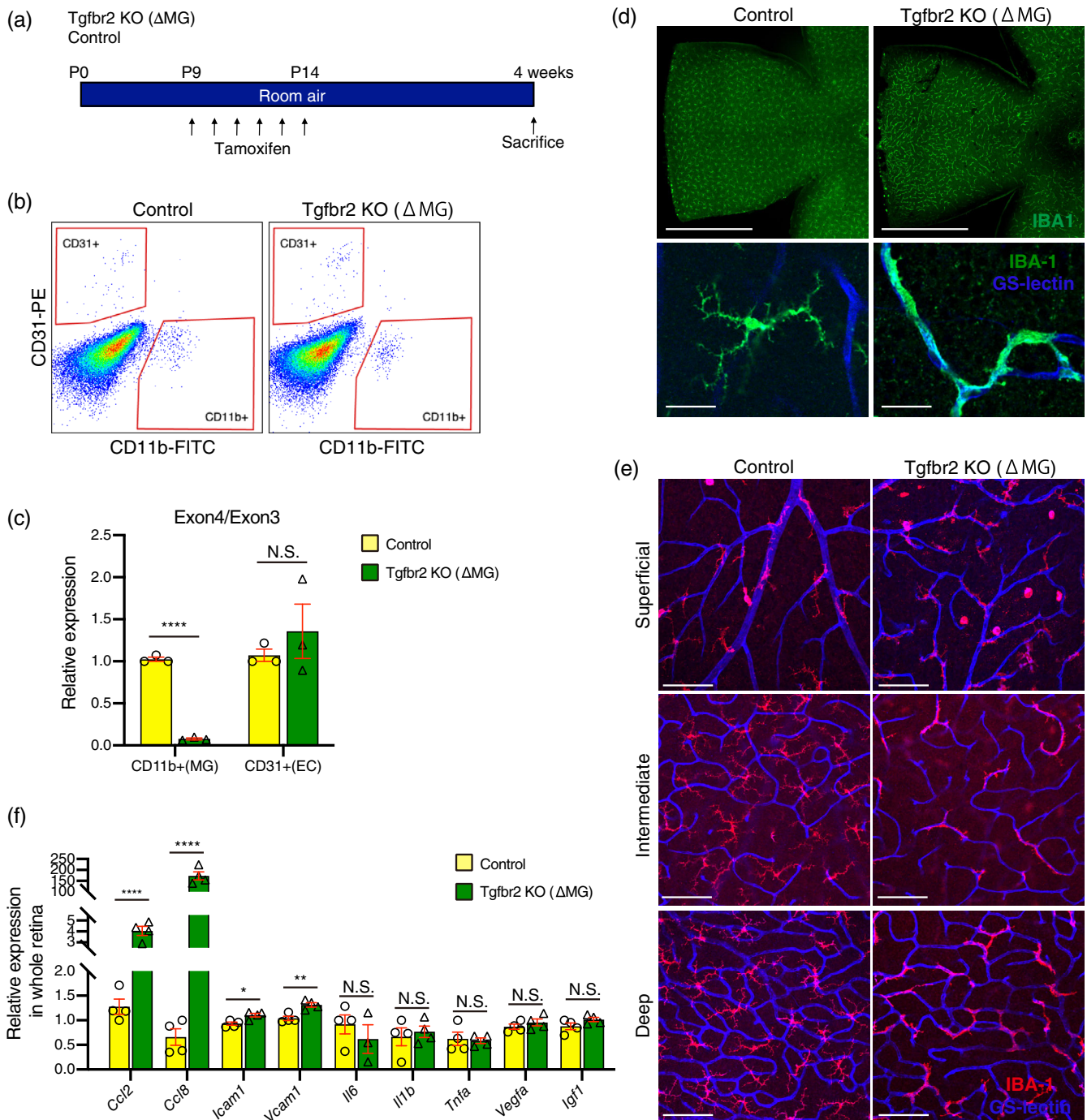


**FIGURE 1** Tgfr2 deficient microglia transform to an activated state. (a) Schematic showing the protocol was used to generate data for Figure 1. (b) the representative flow sorting chart for isolating retinal Cd31 positive endothelial cells and Cd11b positive microglia from control (left) and Tgfr2 KO ( $\Delta$ MG) (right) mice 4 weeks after tamoxifen administration. (c) the ratio of exon3 to exon4 expression in Tgfr2 was determined by qPCR in Cd11b + microglia (MG) or Cd31+ endothelial cells (EC). The expression of exon4 was specifically inhibited in microglia ( $n = 3$  each). Data are mean  $\pm$  SEM.  $p$  Values were calculated using a two-tailed Student's  $t$ -test, \*\*\*\* $p < .0001$ . N.S., not significant. (d) Retinal flatmount stained with IBA1 to visualize microglia 4 weeks after tamoxifen administration to control and Tgfr2 KO ( $\Delta$ MG) mice. Microglia throughout the retina were observed to be transformed and activated in Tgfr2 KO ( $\Delta$ MG) mice. Upper panel: Low magnification (scale bars = 1 mm). Lower panel: High magnification (scale bars = 50  $\mu$ m). (e) the relation between retinal vessels and microglia at each vessel layer 4 weeks after tamoxifen administration to control and Tgfr2 KO ( $\Delta$ MG) mice (scale bars = 100  $\mu$ m). (f) mRNA expression in retinas from control or Tgfr2 KO ( $\Delta$ MG) mice ( $n = 4$  each). Data are mean  $\pm$  SEM.  $p$  Values were calculated using a multiple  $t$ -test, \* $p < .05$ , \*\* $p < .01$ , \*\*\*\* $p < .0001$ , N.S. = not significant.

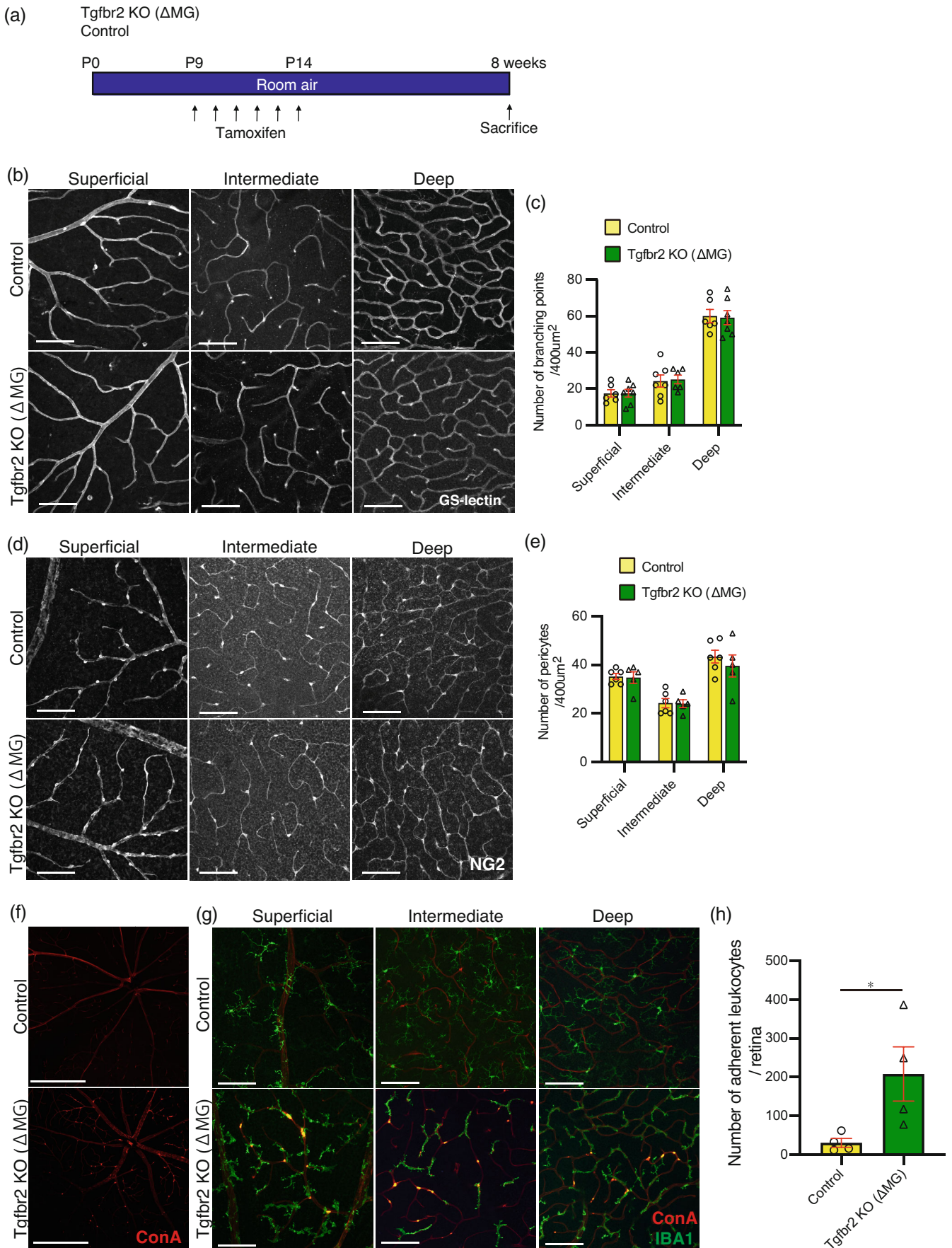
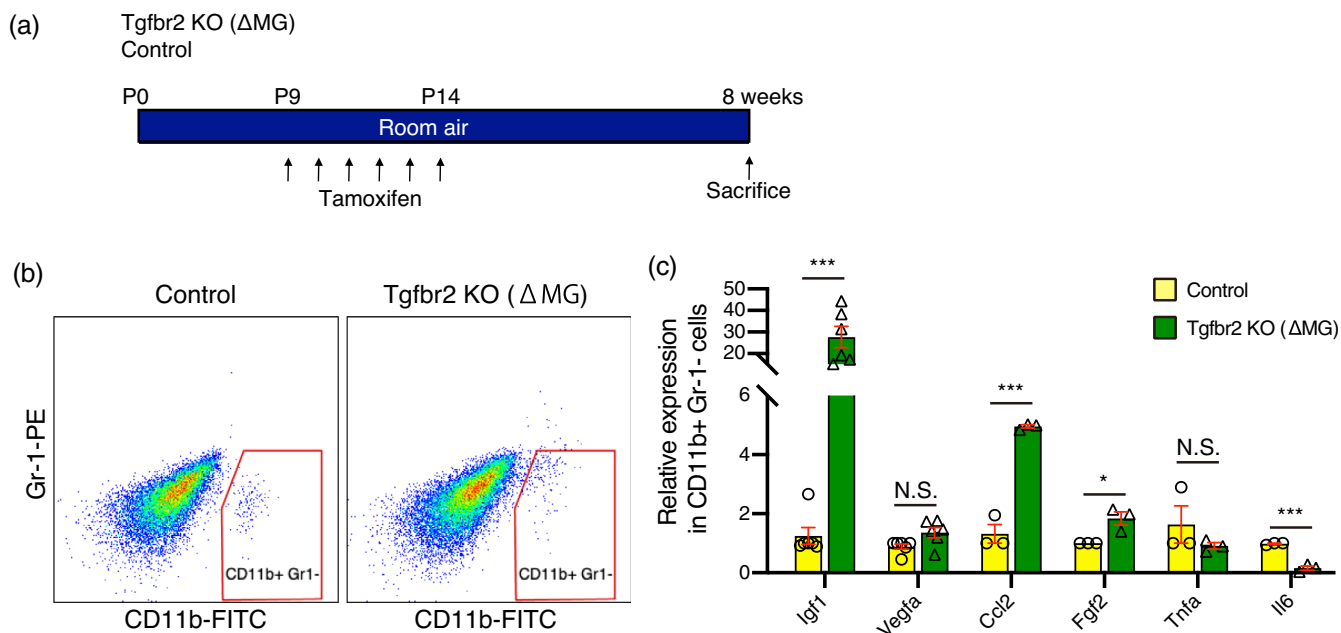


FIGURE 2 Legend on next page.



**FIGURE 3** The proangiogenic factor Igf1 was highly upregulated in Tgfb2 deficient microglia. (a) Schematic showing the protocol used to generate data shown in this figure. (b) Representative flow charts for Cd11b+ Gr-1- microglia sorting in control (left) and Tgfb2 KO (ΔMG) (right) mice. (c) the expression of Igf1, Vegfa, Ccl2, Fgf2, Tnfa, and Il6 in retinal microglia of Tgfb2 KO (ΔMG) or control mice was determined by qPCR (Igf1, and Vegfa:  $n = 6$ , Ccl2, Fgf2, Tnfa, and Il6:  $n = 3$  each). Data are mean  $\pm$  SEM.  $p$ -Values were calculated using a two-tailed Student's  $t$ -test, \* $p < .05$ , \*\*\* $p < .001$ . N.S., not significant.

### 3.3 | Igf1 expression was highly upregulated in Tgfb2 deficient microglia

Next, we examined if Tgfb2 deficient microglia themselves have pro-angiogenic effects. We sorted microglia out from retinal cells by flow cytometry 8 weeks after tamoxifen injection into Tgfb2 KO (ΔMG) and control (Figure 3a) mice. To eliminate circulating and adherent leukocytes, CD11b positive and Gr-1 negative fractions were sorted out from the retina of Tgfb2 KO (ΔMG) and control. The expression of pro-angiogenic genes in the fraction were evaluated by qPCR (Figure 3b). We found that the expression of Igf1, Ccl2, and Fgf2 in microglia from Tgfb2 KO (ΔMG) were significantly higher than microglia from controls (Figure 3c). Among those genes, the expression of Igf1 in microglia from Tgfb2 (ΔMG) was particularly impacted, increasing by 20–50-fold. This demonstrates that knocking out Tgfb2 leads to significantly elevated levels of Igf1, suggesting

that Tgfb signaling is a powerful inhibitor of Igf1 expression in microglia.

### 3.4 | The expression of Tgfb receptors was downregulated and the expression of Igf1 was upregulated specifically in hypoxic microglia of wild type C57BL6 OIR

Numerous studies have shown that Igf1 is associated with pathological NV in proliferative diabetic retinopathy or retinopathy of prematurity (Boulton et al., 1997; Haurigot et al., 2009; Hellstrom et al., 2001; Kondo et al., 2003; Meyer-Schwickerath et al., 1993; Ruberte et al., 2004; Smith et al., 1999; Wilkinson-Berka et al., 2006). Since we have found that Tgfb signaling regulates Igf1 expression in microglia, we next examined the potential regulation of Igf1 in

**FIGURE 2** Tgfb signal deletion in microglia did not affect structure of vessels and vascular development but, promoted the adhesion of leukocytes via enhancing chemoattractant. (a) The schematic shows the protocol that was used to generate data for this figure. (b) GS-lectin labeled retinal vessels at superficial, intermediate, and deep plexus 8 weeks after tamoxifen injection from P9 to P14. Scale bars = 100  $\mu$ m. (c) TRITC-conjugated Concanavalin a (con a) lectin labeled leukocytes adhering to retinal capillary endothelium. Scale bars = 500  $\mu$ m. (d) the number of branching points per 400  $\mu$ m<sup>2</sup> was evaluated (control  $n = 6$ , Tgfb2 KO (ΔMG)  $n = 7$ ). (e) NG2 positive pericytes at superficial, intermediate, and deep plexus 8 weeks after daily tamoxifen injections on P9 to P14 (scale bars = 100  $\mu$ m). (f) the number of NG2 positive pericytes per 400  $\mu$ m<sup>2</sup> was evaluated (control  $n = 6$ , Tgfb2 KO (ΔMG)  $n = 5$ ). (g) TRITC-conjugated Concanavalin a (con a) lectin labeled leukocytes adhering to retinal capillary endothelium (scale bars = 500  $\mu$ m). (h) Adherent leukocytes to retinal capillaries are visualized by TRITC-conjugated con a lectin at each layer. There are more leukocytes in all layers in Tgfb2 KO (ΔMG) mice compared to control (scale bars = 100  $\mu$ m). (i) the number of adherent leukocytes labeled with con a lectin in Tgfb2 KO (ΔMG) mice was higher than those observed in control mice ( $n = 4$  each). Data are mean  $\pm$  SEM.  $p$  Values were calculated using a two-tailed Student's  $t$ -test, \* $p < .05$ .

microglia by Tgf $\beta$  signaling as a retinal angiogenic factor using OIR, the well-established mouse model for studying hypoxia-induced retinal NV (Smith et al., 1994) (Figure 4a). To investigate the interaction between Tgf $\beta$  signal and microglial activation under hypoxia, as well as the relevance of Igf1 in microglia to hypoxia-induced NV, we examined the expression of Tgf $\beta$  receptors and Igf1 in the microglia of hypoxic retinas.

We examined the hypoxia response of the OIR retina at P15, using hypoxyprobe labelling, an indicator of hypoxic conditions in

cells. We chose P15 because NV tufts emerge just after P15 preceded by hypoxic response in OIR retina. Elevated hypoxyprobe labeling shows hypoxia in avascular areas of the OIR retina (Figure 4b). We next determined if Tgf $\beta$ b and Igf1 are altered in hypoxic retinas using qPCR. In whole retina, although the expression of Tgf $\beta$ 1 and Vegfa was significantly upregulated in OIR retina compared to normoxia retina, the expression of Igf1, Tgf $\beta$ br1, and Tgf $\beta$ br2, were comparable between whole retina from OIR and normoxia (Figure 4c). However, the flow-sorted Cd11b positive/Gr-1 negative microglia from C57BL6

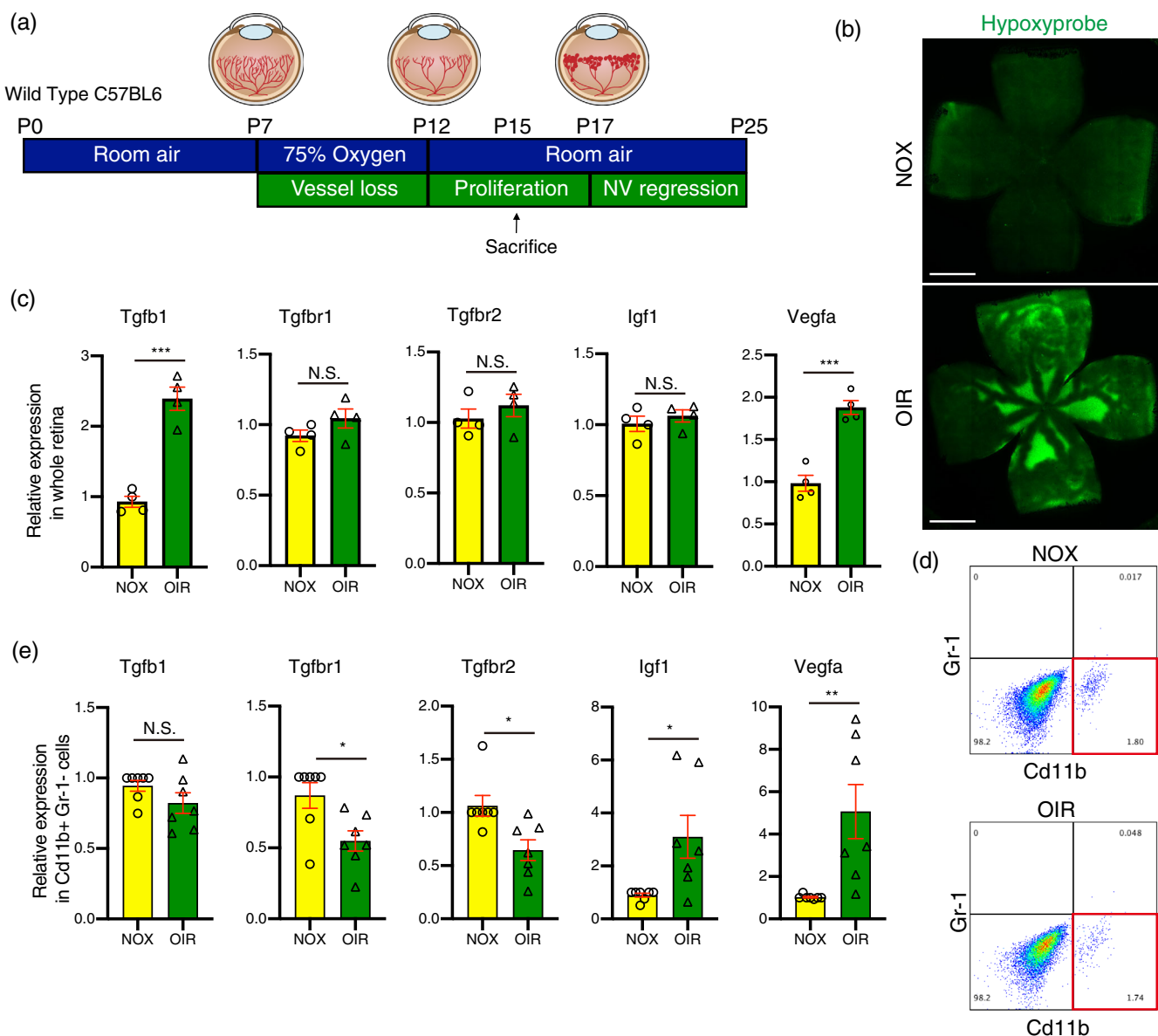


**FIGURE 4** The expression of Tgf $\beta$  receptors was suppressed, and Igf1 upregulated, in hypoxic microglia of oxygen-induced retinopathy (OIR) mice. (a) Schematic showing the protocol used to generate data for the OIR experiment in this figure. (b) The hypoxic retina in P15 OIR mice was detected by Hypoxyprobe-1<sup>TM</sup> (green) (scale bars = 1 mm). (c) The representative flow-sorting scatter stained by Gr-1 and Cd11b. (d) The expression of Tgf $\beta$ 1, Tgf $\beta$ br1, Tgf $\beta$ br2, Igf1, and Vegfa in Cd11b<sup>+</sup> and Gr-1<sup>-</sup> microglia sorted out from P15 OIR and normoxic mice was determined by qPCR ( $n = 7$  each). Data are mean  $\pm$  SEM.  $p$  Values were calculated using a two-tailed Student's  $t$ -test,  $*p < .05$ ,  $**p < .01$ . N.S., not significant. (e) The expression of Tgf $\beta$ 1, Tgf $\beta$ br1, Tgf $\beta$ br2, Igf1, and Vegfa in whole retina from P15 OIR and normoxic mice was determined by qPCR ( $n = 4$  each). Data are mean  $\pm$  SEM.  $p$  Values were calculated using a two-tailed Student's  $t$ -test,  $***p < .001$ . N.S., not significant.



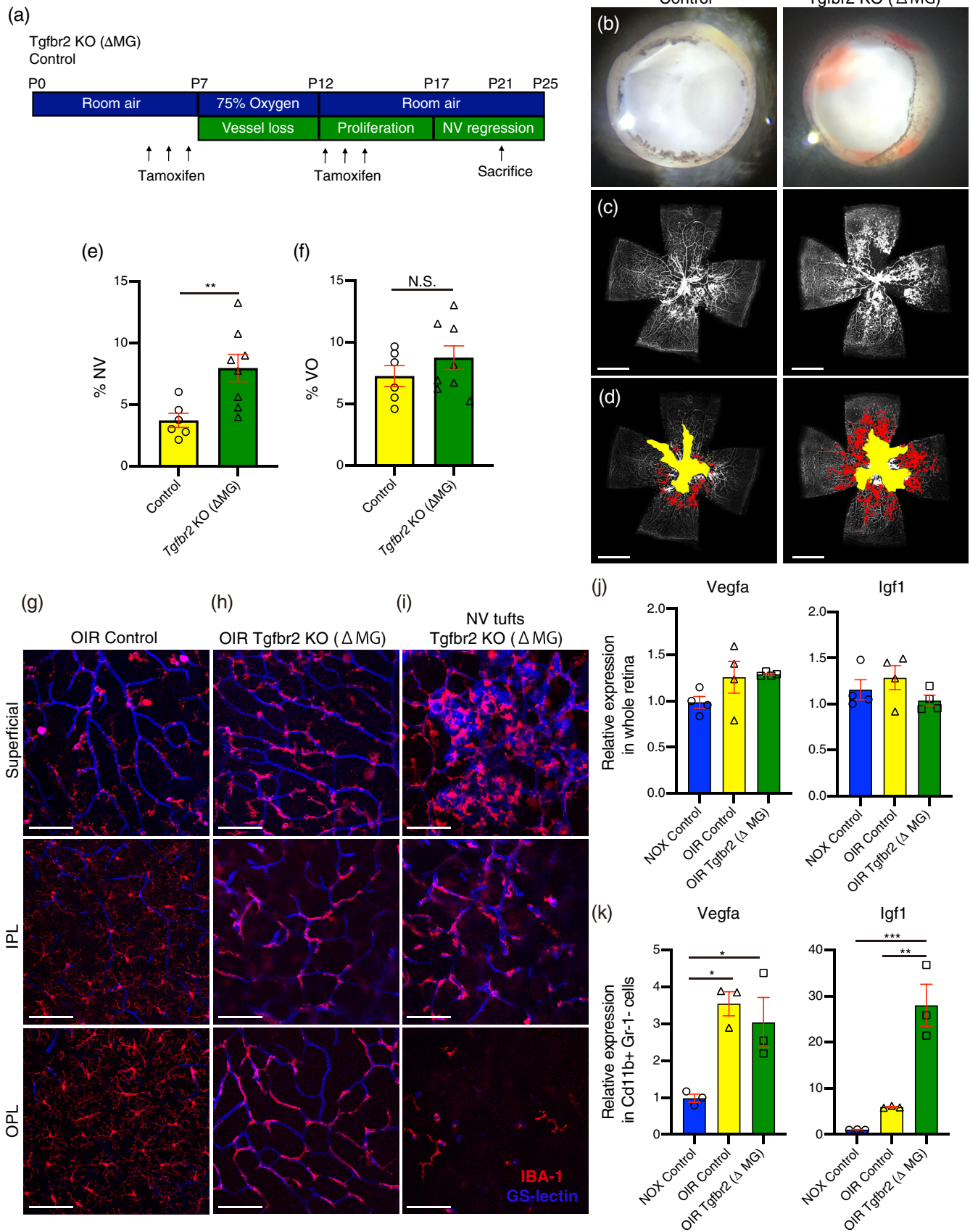


FIGURE 5 Legend on next page.

OIR retina showed significantly higher expression of Igf1 as well as Vegfa compared to normoxia control retinas. OIR microglia also showed lower expression of Tgfb $\beta$ 1 and Tgfb $\beta$ 2, suggesting that the expression of Igf1, and Tgfb $\beta$  receptors, Tgfb $\beta$ 1 and Tgfb $\beta$ 2 were uniquely altered in hypoxic microglia in OIR (Figure 4d,e).

### 3.5 | The blockage of Tgfb $\beta$ signal in microglia exacerbated and prolonged activation of pathological NV in the OIR

Next, we examined if the deletion of Tgfb $\beta$  signal in microglia exacerbated hypoxia induced retinal NVs in OIR. In the OIR model the retina usually shows NV regression and vessel regrowth in the area of vasoobliteration (VO) following P17, when VO is at its peak (Ma & Li, 2021) (Figure 5a). To investigate the role of microglial Tgfb $\beta$  signaling in hypoxia-induced retinal NV, we utilized the OIR model in Tgfb $\beta$ 2 KO ( $\Delta$ MG) mice. At P21, when the OIR usually shows NV regression (Figure 5a), we detected retinal hemorrhaging and a significant increase in NV in Tgfb $\beta$ 2 ( $\Delta$ MG) compared to wildtype OIR controls (Figure 5a–e), whereas the area of VO was unchanged between the two groups. As with Tgfb $\beta$ 2 KO ( $\Delta$ MG) in normoxia, the retinal microglia in Tgfb $\beta$ 2 KO ( $\Delta$ MG) in OIR at p21 were also altered and adhered to vessels in all three layers (Superficial, IPL, and OPL) (Figure 5g,h). At the region of NV tufts that develop in OIR, a large number of activated microglia adhered to NV (Figure 5i), suggesting that the Tgfb $\beta$ 2 deficient microglia exacerbated and prolonged activation of pathological NV in OIR. We next examined the expression level of Vegfa and Igf1 in retina of Tgfb $\beta$ 2 KO ( $\Delta$ MG) OIR compared to control OIR, and control normoxic mice at p21. Unlike the OIR retina at p15, the expression of Vegfa is no longer upregulated in OIR at p21 in the whole retina. In normoxic controls, OIR, and Tgfb $\beta$ 2 KO ( $\Delta$ MG) OIR, Vegfa and Igf1 were comparable between each group (Figure 5j). Similar to OIR at p15 when we isolated Cd11b positive/Gr-1 negative microglia using flow sorting we found that both Vegfa and Igf1 expression were still increased in OIR compared to control (Figure 5k). However only Igf1 expression is exacerbated in Tgfb $\beta$ 2 KO ( $\Delta$ MG) OIR compared to wildtype OIR. Vegfa expression was not changed between Tgfb $\beta$ 2 KO ( $\Delta$ MG) OIR and control OIR microglia (Figure 5k).

### 3.6 | Tgfb $\beta$ 1 regulates Igf1 expression in human iPS cell-derived microglia precursor cells

To validate the regulation of Igf1 expression by Tgfb $\beta$  signal and hypoxia in microglia, we utilized human microglia precursor cells derived from human iPS cells (pMG) according to the well-established protocol from Haenseler et al. (2017). The hiPSC derived microglia precursor cells from this protocol have previously been validated to develop in an MYB-independent, RUNX1-, and PU.1-dependent fashion, consistent with in vivo microglia development (Buchrieser et al., 2017; Prinz & Priller, 2014). We validated pMG using qPCR, flow cytometry, and immunohistochemistry. These cells highly expressed microglia specific markers P2ry12 and Tmem119 as well as macrophage/microglia marker Cd11b by qPCR compared to HUVEC or PBMC (Figure S1a). Flow cytometry showed expression of CD45 (a pan-leukocyte marker), CD14 (a component of the receptor for bacterial lipopolysaccharide), CX3CR1 (fractalkine receptor), and Cd11b on pMGs as previously reported (Figure S1b). Immunocytochemistry also showed that CD45, CD14, IBA1 (microglia/macrophage-specific calcium binding protein), P2RY12, and PU.1 (myeloid transcription factor) were also expressed in pMG (Figure S1c).

We next validated the suppression of Igf1 by Tgfb $\beta$  signaling in human pMGs using Tgfb $\beta$  ligand and Tgfb $\beta$  signaling inhibitors. Twenty four hours following the addition of human recombinant Tgfb $\beta$ 1 to pMG culture media, the expression of Igf1 mRNA in pMG was significantly suppressed as expected (Figure 6a). We subsequently confirmed that IGF1 protein secreted into media was also suppressed by human recombinant Tgfb $\beta$ 1 (Figure 6b). Conversely, addition of the Tgfb $\beta$ 2 inhibitor, SB525334, to pMGs increased Igf1 expression and was sufficient to rescue Igf1 suppression in the presence of Tgfb $\beta$ 1 (Figure 6c). Vegfa expression in pMG was not changed by Tgfb $\beta$ 1 or SB525334 (Figure 6d). Next, to determine if hypoxic conditions could regulate the expression of Igf1 in pMG, we utilized the hypoxia mimetic Dimethylxylglycine (DMOG), which stabilizes hypoxia inducible factor-1 $\alpha$  (HIF-1 $\alpha$ ). Vegfa, which is a direct target of HIF-1 $\alpha$ , showed a large and significant increase in expression in pMGs following 24 h of DMOG treatment which tapered off by 48 h (Figure 6f). However, Igf1 expression in pMG was not upregulated

**FIGURE 5** The blockage of Tgfb $\beta$  signal in microglia exacerbate and prolong activation of pathological neovascularization (NV) in oxygen induced retinopathy (OIR). (a) Schematic showing the protocol used to generate data shown in the OIR experiment. The area of NV and vasoobliteration (VO) were analyzed at P21 when the OIR usually shows NV regression after its peak at P17. (b) Representative retinal cups from P21 OIR. Retinal hemorrhage was detected in retinas from Tgfb $\beta$ 2 KO ( $\Delta$ MG) mice. (c) Retinal flat mount at P21 OIR stained with fluorescein-conjugated isolectin Griffonia simplicifolia IB-4 (GS-lectin) for retinal vessels. (d) The area of NV pseudocolored in red and the area of VO pseudocolored in yellow (scale bars = 1 mm). (e, f) The quantification of NV (d) and VO (f) areas (control  $n = 6$ , Tgfb $\beta$ 2 KO ( $\Delta$ MG)  $n = 8$ ). Data are mean  $\pm$  SEM.  $p$  Values were calculated using a two-tailed Student's  $t$ -test, \*\* $p < .01$ , N.S., not significant. (g–i) Microglia and retinal vessels were visualized by immunostaining of IBA1 (red) and GS-lectin (blue), respectively, in control (g), vascularized parts of Tgfb $\beta$ 2 KO ( $\Delta$ MG) (h), and neovascular tuft of Tgfb $\beta$ 2 KO ( $\Delta$ MG) (i) at each retinal layer. Microglia from Tgfb $\beta$ 2 KO ( $\Delta$ MG) tightly adhered to superficial, intermediate, deep plexus as well as neovascular tufts. IPL, inner plexiform layer, OPL, outer plexiform layer, NV tufts, neovascular tufts. Scale bars = 100  $\mu$ m. (j) The expression of Vegfa and Igf1 in whole retina from normoxic (NOX) control, OIR control, and Tgfb $\beta$ 2 KO ( $\Delta$ MG) OIR ( $n = 4$  each). Data are mean  $\pm$  SEM. (k) The expression of Vegfa and Igf1 in Cd11b+ Gr-1- microglial cells from NOX control, OIR control, and Tgfb $\beta$ 2 KO ( $\Delta$ MG) OIR. Mice ( $n = 3$  each). Data are mean  $\pm$  SEM.  $p$  Values were calculated using ordinary one-way ANOVA and Tukey's multiple comparison test. \* $p < .05$ , \*\* $p < .01$ , \*\*\* $p < .001$ .

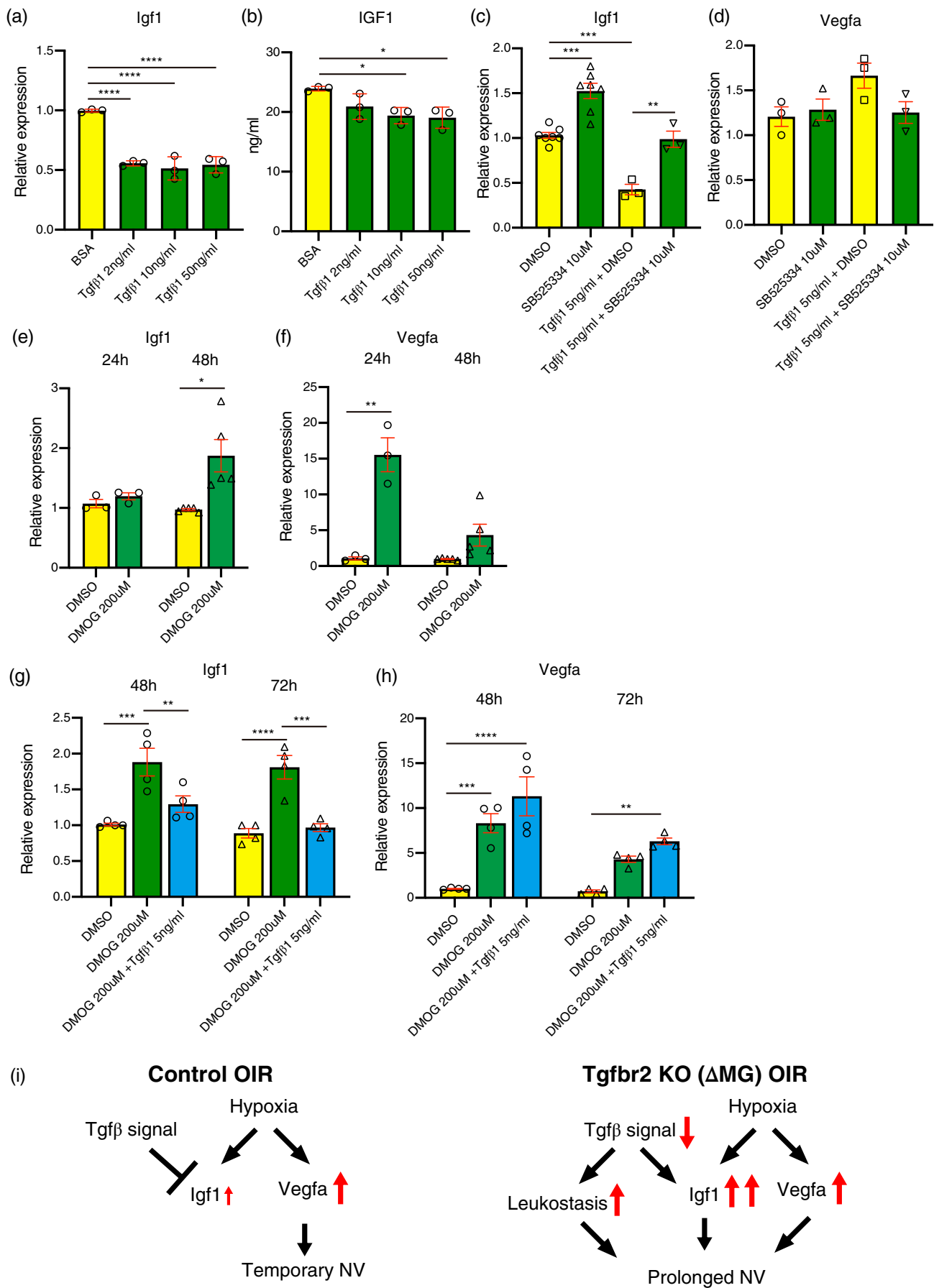


**FIGURE 6** Legend on next page.

following 24 h of DMOG treatment and only showed a significant increase in expression at 48 h indicating that it is not directly induced by HIF-1 $\alpha$  (Figure 6e). Next, we looked at the interaction between hypoxia and Tgfb signaling on Igf1 regulation and found that human recombinant Tgfb1 rescued hypoxia induced Igf1 upregulation (Figure 6g), but had no effect on hypoxia induced Vegfa upregulation (Figure 6h).

## 4 | DISCUSSION

We have demonstrated that Tgfb signal in microglia played a role in regulating microglia homeostasis; inhibiting it resulted in exacerbating pathological NV through the upregulation of Igf1 in a mouse model of ischemic retinopathy.

Microglia are resident immune cells in the central nervous system. Under healthy conditions, retinal microglia are mainly localized in the outer and inner plexiform layer and superficial plexus where they engage in surveillance and maintenance of retinal synapses (Lee et al., 2008; Wang et al., 2016). However, under pathological conditions such as retinal degeneration, neovascularization and aging, microglia activate and migrate into the sites where those pathological changes occur. They also localize to damaged photoreceptors, RPE, and retinal or choroidal NV (Ma et al., 2009; Usui-Ouchi et al., 2020; Zhao et al., 2015). Given this association between activated/primed microglia and neurovasculodegenerative diseases, it is necessary to better understand activation mechanisms in microglia.

Tgfb signaling has pleiotropic effects in various tissues on cell survival and inflammation (Travis & Sheppard, 2014). In mammals, the Tgfb family consists of three members, Tgfb1, Tgfb2, and Tgfb3, and all isoforms can be detected in various types of ocular cells including retinal neurons, retinal pigment epithelium, blood vessels, and microglia (Tosi et al., 2018). Tgfb receptors are also broadly expressed in different retinal cell types, specifically, in retinal microglia and endothelial cells (Ma et al., 2019; Obata et al., 1999). Deletion of panocular Tgfb signaling leads to proliferative diabetic retinopathic changes such as pericyte loss, the formation of abundant microaneurysms, leaky capillaries, and retinal hemorrhages (Braunger

et al., 2015). Tgfb1 has previously been described as a potent immunoregulatory factor for cerebral microglia in vivo and in vitro (Brionne et al., 2003; Makwana et al., 2007; Spittau et al., 2013; Zoller et al., 2018). As for retinal microglia, Ma et al. demonstrated that ablation of Tgfb2 in retinal microglia induced their activation as well as the promotion of pathological microglia gene expression profiles resulting in secondary Muller cell gliosis, neuronal apoptosis, and abnormal synaptic transmission (Ma et al., 2019). We have also detected activated pathological microglia in our microglia specific Tgfb2 knockout mice although we used a different Cre induction protocol with Tamoxifen. Ma and colleagues also reported that Tgfb2 deficient microglia demonstrated an exaggerated response to laser-induced choroidal NV (Ma et al., 2019). However, the mechanism whereby Tgfb signaling in microglia led to choroidal NV formation was not well defined.

Activated microglia cells are found in the central avascular zone of retinas with ischemic retinopathy (Fischer et al., 2011; Vessey et al., 2011). Pharmacological microglia depletion rescues pathological NV in OIR (Kubota et al., 2009), indicating that retinal microglia may be involved in retinal NV in hypoxic retinas. Moreover, Boeck et al. recently demonstrated, using cell-specific reporter mice, that microglia are the predominant myeloid cell population in areas of retinal NV in OIR. Macrophages rarely appear in these areas. Furthermore, activated retinal microglia alter their transcriptional profile and exhibit considerable proliferative ability (Boeck et al., 2020). However, the mechanism by which microglia become activated and promote NV under hypoxia has not been defined. In this study, we report the influence of retinal microglial Tgfb signaling on retinal NV and its mechanism during the hypoxic response.

We have shown microglia in the avascular area of OIR are hypoxic and those cells express lower Tgfb1 and higher Igf1 than those in normoxic healthy retina. This suggests that lacking Tgfb signal and Igf1 upregulation in microglia could exaggerate Vegfa induced pro-angiogenic response under hypoxia. Using the immortalized rodent microglia cell line BV-2, Yin et al. showed hypoxic microglia produce Igf1, increasing their pro-angiogenic capacity (Yin et al., 2017). We demonstrated that chemical-induced hypoxia upregulated Igf1 expression. Moreover, the upregulation of Igf1 was also rescued

**FIGURE 6** Tgfb1 regulates Igf1 expression in human iPSCs derived microglia. (a) Igf1 expression was downregulated with 2, 10, 50 ng/ml of human recombinant Tgfb1 24 h after supplementation ( $n = 3$ ). Data are mean  $\pm$  SEM.  $p$  Values were calculated using ordinary one-way ANOVA and Tukey's multiple comparison test. \*\*\*\* $p < .0001$ . (b) the protein concentration of IGF1 in the supernatant of human iPSCs derived microglia was determined by ELISA and downregulated after human recombinant Tgfb1 supplementation ( $n = 3$ ). Data are mean  $\pm$  SEM.  $p$  Values were calculated using ordinary one-way ANOVA and Tukey's multiple comparison test. \* $p < .05$ . (c, d) Relative Igf1 (c) and Vegfa (d) expression levels were determined by qPCR 48 h after supplementation. 10  $\mu$ M of SB525334, Tgfb2 inhibitor induced Igf1 expression and SB525334 inhibited Tgfb1 induced Igf1 downregulation (DMSO and SB525334:  $n = 7$ , Tgfb1 + DMSO and Tgfb1 + SB525334:  $n = 3$ ). Data are mean  $\pm$  SEM.  $p$  Values were calculated using ordinary one-way ANOVA and Tukey's multiple comparison test. \*\* $p < .01$ , \*\*\* $p < .001$ . (e, f) 200  $\mu$ M of dimethylallyl glycine (DMOG) was supplemented to induce chemical hypoxia in hiPSC derived microglia and the expression of Igf1 (e) and Vegfa (f) were evaluated at 24 and 48 h after the treatments (24 h:  $n = 3$  each, 48 h:  $n = 5$  each) data are mean  $\pm$  SEM.  $p$  Values were calculated using a two-tailed Student's  $t$ -test, \* $p < .05$ , \*\* $p < .01$ . (g, h) 5 ng/ml Tgfb1 rescued DMOG induced Igf1 (g) upregulation, but not Vegfa (h) upregulation at 48 and 72 h after the treatments ( $n = 4$  each). Data are mean  $\pm$  SEM.  $p$  Values were calculated using ordinary one-way ANOVA and Tukey's multiple comparison test. \*\* $p < .01$ , \*\*\* $p < .001$ , \*\*\*\* $p < .0001$ . (i) The schema shows the relationship between Tgfb signal and hypoxia-induced retinal neovascularization in retinal microglia from control OIR or Tgfb2 KO ( $\Delta$ MG) OIR.

by Tgfb1 supplementation, suggesting that Tgfb1 regulates hypoxia-induced Igf1 upregulation in microglia.

We also report that Tgfb2 ablation in microglia exacerbated pathological NV in OIR. We found two remarkable changes that could exacerbate pathological NV: (1) an increase in retinal leukostasis in retinal capillaries through production of chemoattractant factors; and (2) an increase in Igf1 expression in microglia. Retinal leukostasis indicates an increase in leukocyte recruitment and adhesion to the retinal capillary endothelium. Retinal leukostasis can lead to blood-retinal barrier breakdown, capillary occlusion, and amplification of the inflammatory response in various retinal diseases such as diabetic retinopathy, ischemic retinopathy, and uveitis (Eshaq et al., 2017; Tarr et al., 2013; Tsujikawa & Ogura, 2012). Dysregulated microglia caused by Tgfb2 ablation were closely adherent to retinal vessels and produced chemoattractant factors such as Ccl2 and Ccl8, chemokines that can lead to the recruitment of circulating monocytes, promoting pathological NV.

Numerous studies have shown that Igf1 is associated with pathological NV in proliferative diabetic retinopathy or retinopathy of prematurity (Boulton et al., 1997; Haurigot et al., 2009; Hellstrom et al., 2001; Kondo et al., 2003; Meyer-Schwickerath et al., 1993; Ruberte et al., 2004; Smith et al., 1999; Wilkinson-Berka et al., 2006). For example, IGF1 is required for maximal VEGF-dependent NV via the IGF1 receptor and MAPK activation in OIR, and Igf1 knockout mice had impaired retinal vascular growth despite normal VEGF level (Smith et al., 1999). Jacobo et al demonstrated that IGF1 stabilizes endothelial cell tubes and retinal neovessels that form in response to VEGF, mediating prolonged activation of Erk, which antagonizes lysophosphatidic acid (LPA)-driven regression (Jacobo & Kazlauskas, 2015). Endothelial cell specific IGF1 receptor KO mice show reduced retinal NV in OIR (Kondo et al., 2003). On the other hand, overexpression of IGF1 in the retina results in changes similar to those of diabetic retinopathy (pericyte loss, capillary basement membrane thickness, inner retinal microaneurysms, and neovessels) (Ruberte et al., 2004). Patients with proliferative diabetic retinopathy have increased vitreous levels of IGF1 (Boulton et al., 1997; Grant et al., 1986; Meyer-Schwickerath et al., 1993). Thus, although IGF1 plays a key role in pathological NV in retina, the origin of IGF1 and interaction between endothelial cell and microglia in the retinal microenvironment has not been well defined. Our results support the idea that IGF1 in diabetic retinopathy or retinopathy of prematurity may be derived from retinal microglia. We further suggest that abundant IGF1 produced by activated microglia stabilizes VEGF-driven retinal neovessels resulting in the exacerbation and prolonged pathological NV in Tgfb2 KO ( $\Delta$ MG) OIR.

We have also shown that Tgfb1-regulated Igf1 expression using hiPS derived microglia cells and Tgfb1 rescued Igf1 upregulation under chemically induced hypoxia. We surmised Igf1 upregulation in hypoxic microglia induces retinal NVs synergistically with hypoxia induced Vegfa upregulation. Igf1 upregulation after hypoxia occurred at alter time than Vegfa upregulation, suggesting that Igf1 released by hypoxic microglia plays an important role in stabilizing and prolonging pathological NV induced by Vegfa under hypoxia.

Collectively, these results demonstrate that Tgfb signaling in retinal microglia is critical for maintaining their homeostatic function and regulation of their hypoxic response in ischemic retinopathy. Targeting Tgfb signaling in microglia may be a potential therapeutic target to treat pathological NVs in ischemic retinopathy.

## ACKNOWLEDGMENTS

We thank the members of the Friedlander laboratory at Scripps Research and our colleagues at the Lowy Medical Research Institute for many helpful discussions regarding the direction of this project and the data presented in this manuscript. We would like to thank the TSRI's Flow cytometry core for their excellent technical assistance, and the TSRI's animal vivarium staff for the excellent care of the animals used in this study. This work was supported by the Lowy Medical Research Institute and NIH grants EY11254 (to M.F.). A.U.-O. is supported by a fellowship from the Manpei Suzuki Diabetes Foundation and JSPS KAKENHI Grant Number 17K16984 and 21K09727.

## CONFLICT OF INTEREST

The authors declare no conflict of interest.

## DATA AVAILABILITY STATEMENT

The data that support the findings of this study are available from the corresponding author upon reasonable request.

## ORCID

Ayumi Usui-Ouchi  <https://orcid.org/0000-0003-2974-0830>

Martin Friedlander  <https://orcid.org/0000-0003-4238-9651>

## REFERENCES

- Ashraf, M., Souka, A. A., & Singh, R. P. (2016). Central retinal vein occlusion: Modifying current treatment protocols. *Eye (London, England)*, 30(4), 505–514. <https://doi.org/10.1038/eye.2016.10>
- Boeck, M., Thien, A., Wolf, J., Hagemeyer, N., Laich, Y., Yusuf, D., ... Lange, C. (2020). Temporospatial distribution and transcriptional profile of retinal microglia in the oxygen-induced retinopathy mouse model. *GLIA*, 68(9), 1859–1873. <https://doi.org/10.1002/glia.23810>
- Boulton, M., Gregor, Z., McLeod, D., Charteris, D., Jarvis-Evans, J., Moriarty, P., ... Bardsley, B. (1997). Intravitreal growth factors in proliferative diabetic retinopathy: Correlation with neovascular activity and glycaemic management. *The British Journal of Ophthalmology*, 81(3), 228–233. <https://doi.org/10.1136/bjo.81.3.228>
- Braunger, B. M., Leimbeck, S. V., Schlecht, A., Volz, C., Jagle, H., & Tamm, E. R. (2015). Deletion of ocular transforming growth factor beta signaling mimics essential characteristics of diabetic retinopathy. *The American Journal of Pathology*, 185(6), 1749–1768. <https://doi.org/10.1016/j.ajpath.2015.02.007>
- Brionne, T. C., Teseur, I., Masliah, E., & Wyss-Coray, T. (2003). Loss of TGF-beta 1 leads to increased neuronal cell death and microgliosis in mouse brain. *Neuron*, 40(6), 1133–1145. [https://doi.org/10.1016/s0896-6273\(03\)00766-9](https://doi.org/10.1016/s0896-6273(03)00766-9)
- Buchrieser, J., James, W., & Moore, M. D. (2017). Human induced pluripotent stem cell-derived macrophages share ontogeny with MYB-independent tissue-resident macrophages. *Stem Cell Reports*, 8(2), 334–345. <https://doi.org/10.1016/j.stemcr.2016.12.020>
- Butovsky, O., Jedrychowski, M. P., Moore, C. S., Cialic, R., Lanser, A. J., Gabrieli, G., ... Weiner, H. L. (2014). Identification of a unique TGF-beta-dependent molecular and functional signature in microglia.

- Nature Neuroscience*, 17(1), 131–143. <https://doi.org/10.1038/nn.3599>
- Engerman, R. L. (1989). Pathogenesis of diabetic retinopathy. *Diabetes*, 38(10), 1203–1206. <https://doi.org/10.2337/diab.38.10.1203>
- Eshaq, R. S., Aldalati, A. M. Z., Alexander, J. S., & Harris, N. R. (2017). Diabetic retinopathy: Breaking the barrier. *Pathophysiology*, 24(4), 229–241. <https://doi.org/10.1016/j.pathophys.2017.07.001>
- Falavarjani, K. G., & Nguyen, Q. D. (2013). Adverse events and complications associated with intravitreal injection of anti-VEGF agents: A review of literature. *Eye (London, England)*, 27(7), 787–794. <https://doi.org/10.1038/eye.2013.107>
- Fischer, F., Martin, G., & Agostini, H. T. (2011). Activation of retinal microglia rather than microglial cell density correlates with retinal neovascularization in the mouse model of oxygen-induced retinopathy. *Journal of Neuroinflammation*, 8, 120. <https://doi.org/10.1186/1742-2094-8-120>
- Fogli, S., Del Re, M., Rofi, E., Posarelli, C., Figus, M., & Danesi, R. (2018). Clinical pharmacology of intravitreal anti-VEGF drugs. *Eye (London, England)*, 32(6), 1010–1020. <https://doi.org/10.1038/s41433-018-0021-7>
- Grant, M., Russell, B., Fitzgerald, C., & Merimee, T. J. (1986). Insulin-like growth factors in vitreous. Studies in control and diabetic subjects with neovascularization. *Diabetes*, 35(4), 416–420. <https://doi.org/10.2337/diab.35.4.416>
- Haenseler, W., Sansom, S. N., Buchrieser, J., Newey, S. E., Moore, C. S., Nicholls, F. J., ... Cowley, S. A. (2017). A highly efficient human pluripotent stem cell microglia model displays a neuronal-co-culture-specific expression profile and inflammatory response. *Stem Cell Reports*, 8(6), 1727–1742. <https://doi.org/10.1016/j.stemcr.2017.05.017>
- Haurigot, V., Villacampa, P., Ribera, A., Lombart, C., Bosch, A., Nacher, V., ... Bosch, F. (2009). Increased intraocular insulin-like growth factor-I triggers blood-retinal barrier breakdown. *The Journal of Biological Chemistry*, 284(34), 22961–22969. <https://doi.org/10.1074/jbc.M109.014787>
- Hellstrom, A., Perruzzi, C., Ju, M., Engstrom, E., Hard, A. L., Liu, J. L., ... Smith, L. E. (2001). Low IGF-I suppresses VEGF-survival signaling in retinal endothelial cells: Direct correlation with clinical retinopathy of prematurity. *Proceedings of the National Academy of Sciences of the United States of America*, 98(10), 5804–5808. <https://doi.org/10.1073/pnas.101113998>
- Ip, M. S., Domalpally, A., Sun, J. K., & Ehrlich, J. S. (2015). Long-term effects of therapy with ranibizumab on diabetic retinopathy severity and baseline risk factors for worsening retinopathy. *Ophthalmology*, 122(2), 367–374. <https://doi.org/10.1016/j.ophtha.2014.08.048>
- Jacobo, S. M., & Kazlauskas, A. (2015). Insulin-like growth factor 1 (IGF-1) stabilizes nascent blood vessels. *The Journal of Biological Chemistry*, 290(10), 6349–6360. <https://doi.org/10.1074/jbc.M114.634154>
- Joussen, A. M., Murata, T., Tsujikawa, A., Kirchhof, B., Bursell, S. E., & Adamis, A. P. (2001). Leukocyte-mediated endothelial cell injury and death in the diabetic retina. *The American Journal of Pathology*, 158(1), 147–152. [https://doi.org/10.1016/S0002-9440\(10\)63952-1](https://doi.org/10.1016/S0002-9440(10)63952-1)
- Kondo, T., Vicent, D., Suzuma, K., Yanagisawa, M., King, G. L., Holzenberger, M., & Kahn, C. R. (2003). Knockout of insulin and IGF-1 receptors on vascular endothelial cells protects against retinal neovascularization. *The Journal of Clinical Investigation*, 111(12), 1835–1842. <https://doi.org/10.1172/JCI17455>
- Kubota, Y., Takubo, K., Shimizu, T., Ohno, H., Kishi, K., Shibuya, M., ... Suda, T. (2009). M-CSF inhibition selectively targets pathological angiogenesis and lymphangiogenesis. *The Journal of Experimental Medicine*, 206(5), 1089–1102. <https://doi.org/10.1084/jem.20081605>
- Lee, J. E., Liang, K. J., Fariss, R. N., & Wong, W. T. (2008). Ex vivo dynamic imaging of retinal microglia using time-lapse confocal microscopy. *Investigative Ophthalmology & Visual Science*, 49(9), 4169–4176. <https://doi.org/10.1167/iovs.08-2076>
- Leveen, P., Larsson, J., Ehinger, M., Cilio, C. M., Sundler, M., Sjostrand, L. J., ... Karlsson, S. (2002). Induced disruption of the transforming growth factor beta type II receptor gene in mice causes a lethal inflammatory disorder that is transplantable. *Blood*, 100(2), 560–568. <https://doi.org/10.1182/blood.v100.2.560>
- Ma, W., Silverman, S. M., Zhao, L., Villasmil, R., Campos, M. M., Amaral, J., & Wong, W. T. (2019). Absence of TGFbeta signaling in retinal microglia induces retinal degeneration and exacerbates choroidal neovascularization. *eLife*, 8, e42049. <https://doi.org/10.7554/eLife.42049>
- Ma, W., Zhao, L., Fontainhas, A. M., Fariss, R. N., & Wong, W. T. (2009). Microglia in the mouse retina alter the structure and function of retinal pigmented epithelial cells: A potential cellular interaction relevant to AMD. *PLoS One*, 4(11), e7945. <https://doi.org/10.1371/journal.pone.0007945>
- Ma, Y., & Li, T. (2021). Monitoring dynamic growth of retinal vessels in oxygen-induced retinopathy mouse model. *Journal of Visualized Experiments*, 170, 62410. <https://doi.org/10.3791/62410>
- Makwana, M., Jones, L. L., Cuthill, D., Heuer, H., Bohatschek, M., Hristova, M., ... Raivich, G. (2007). Endogenous transforming growth factor beta 1 suppresses inflammation and promotes survival in adult CNS. *The Journal of Neuroscience*, 27(42), 11201–11213. <https://doi.org/10.1523/JNEUROSCI.2255-07.2007>
- Meyer-Schwickerath, R., Pfeiffer, A., Blum, W. F., Freyberger, H., Klein, M., Losche, C., ... Schatz, H. (1993). Vitreous levels of the insulin-like growth factors I and II, and the insulin-like growth factor binding proteins 2 and 3, increase in neovascular eye disease. Studies in nondiabetic and diabetic subjects. *The Journal of Clinical Investigation*, 92(6), 2620–2625. <https://doi.org/10.1172/JCI116877>
- Murinello, S., Usui, Y., Sakimoto, S., Kitano, M., Aguilar, E., Friedlander, H. M., ... Friedlander, M. (2019). miR-30a-5p inhibition promotes interaction of Fas(+) endothelial cells and FasL(+) microglia to decrease pathological neovascularization and promote physiological angiogenesis. *Glia*, 67(2), 332–344. <https://doi.org/10.1002/glia.23543>
- Obata, H., Kaji, Y., Yamada, H., Kato, M., Tsuru, T., & Yamashita, H. (1999). Expression of transforming growth factor-beta superfamily receptors in rat eyes. *Acta Ophthalmologica Scandinavica*, 77(2), 151–156. <https://doi.org/10.1034/j.1600-0420.1999.770207.x>
- Okunuki, Y., Mukai, R., Nakao, T., Tabor, S. J., Butovsky, O., Dana, R., ... Connor, K. M. (2019). Retinal microglia initiate neuroinflammation in ocular autoimmunity. *Proceedings of the National Academy of Sciences of the United States of America*, 116(20), 9989–9998. <https://doi.org/10.1073/pnas.1820387116>
- Parkhurst, C. N., Yang, G., Ninan, I., Savas, J. N., Yates, J. R., 3rd, Lafaille, J. J., ... Gan, W. B. (2013). Microglia promote learning-dependent synapse formation through brain-derived neurotrophic factor. *Cell*, 155(7), 1596–1609. <https://doi.org/10.1016/j.cell.2013.11.030>
- Prinz, M., & Priller, J. (2014). Microglia and brain macrophages in the molecular age: From origin to neuropsychiatric disease. *Nature Reviews. Neuroscience*, 15(5), 300–312. <https://doi.org/10.1038/nrn3722>
- Ruberte, J., Ayuso, E., Navarro, M., Carretero, A., Nacher, V., Haurigot, V., ... Bosch, F. (2004). Increased ocular levels of IGF-1 in transgenic mice lead to diabetes-like eye disease. *The Journal of Clinical Investigation*, 113(8), 1149–1157. <https://doi.org/10.1172/JCI19478>
- Silverman, S. M., & Wong, W. T. (2018). Microglia in the retina: Roles in development, maturity, and disease. *Annual Review of Vision Science*, 4, 45–77. <https://doi.org/10.1146/annurev-vision-091517-034425>
- Smith, L. E., Shen, W., Perruzzi, C., Soker, S., Kinose, F., Xu, X., ... Senger, D. R. (1999). Regulation of vascular endothelial growth factor-dependent retinal neovascularization by insulin-like growth factor-1 receptor. *Nature Medicine*, 5(12), 1390–1395. <https://doi.org/10.1038/70963>
- Smith, L. E., Wesolowski, E., McLellan, A., Kostyk, S. K., D'Amato, R., Sullivan, R., & D'Amore, P. A. (1994). Oxygen-induced retinopathy in

- the mouse. *Investigative Ophthalmology & Visual Science*, 35(1), 101–111. <https://www.ncbi.nlm.nih.gov/pubmed/7507904>
- Spittau, B., Wullkopf, L., Zhou, X., Rilka, J., Pfeifer, D., & Kriegstein, K. (2013). Endogenous transforming growth factor-beta promotes quiescence of primary microglia in vitro. *Glia*, 61(2), 287–300. <https://doi.org/10.1002/glia.22435>
- Tarr, J. M., Kaul, K., Chopra, M., Kohner, E. M., & Chibber, R. (2013). Pathophysiology of diabetic retinopathy. *ISRN Ophthalmology*, 2013, 343560. <https://doi.org/10.1155/2013/343560>
- Tosi, G. M., Orlandini, M., & Galvagni, F. (2018). The controversial role of TGF-beta in Neovascular age-related macular degeneration pathogenesis. *International Journal of Molecular Sciences*, 19(11), 3363. <https://doi.org/10.3390/ijms19113363>
- Travis, M. A., & Sheppard, D. (2014). TGF-beta activation and function in immunity. *Annual Review of Immunology*, 32, 51–82. <https://doi.org/10.1146/annurev-immunol-032713-120257>
- Tsujikawa, A., & Ogura, Y. (2012). Evaluation of leukocyte-endothelial interactions in retinal diseases. *Ophthalmologica*, 227(2), 68–79. <https://doi.org/10.1159/000332080>
- Usui, Y., Westenskow, P. D., Murinello, S., Dorrell, M. I., Schepke, L., Bucher, F., ... Friedlander, M. (2015). Angiogenesis and eye disease. *Annual Review of Vision Science*, 1, 155–184. <https://doi.org/10.1146/annurev-vision-082114-035439>
- Usui-Ouchi, A., & Friedlander, M. (2019). Anti-VEGF therapy: Higher potency and long-lasting antagonism are not necessarily better. *The Journal of Clinical Investigation*, 129(8), 3032–3034. <https://doi.org/10.1172/JCI129862>
- Usui-Ouchi, A., Usui, Y., Kurihara, T., Aguilar, E., Dorrell, M. I., Ideguchi, Y., ... Friedlander, M. (2020). Retinal microglia are critical for subretinal neovascular formation. *JCI Insight*, 5(12), e137317. <https://doi.org/10.1172/jci.insight.137317>
- van Wilgenburg, B., Browne, C., Vowles, J., & Cowley, S. A. (2013). Efficient, long term production of monocyte-derived macrophages from human pluripotent stem cells under partly-defined and fully-defined conditions. *PLoS One*, 8(8), e71098. <https://doi.org/10.1371/journal.pone.0071098>
- Vessey, K. A., Wilkinson-Berka, J. L., & Fletcher, E. L. (2011). Characterization of retinal function and glial cell response in a mouse model of oxygen-induced retinopathy. *The Journal of Comparative Neurology*, 519(3), 506–527. <https://doi.org/10.1002/cne.22530>
- Wang, X., Zhao, L., Zhang, J., Fariss, R. N., Ma, W., Kretschmer, F., ... Wong, W. T. (2016). Requirement for microglia for the maintenance of synaptic function and integrity in the mature retina. *The Journal of Neuroscience*, 36(9), 2827–2842. <https://doi.org/10.1523/JNEUROSCI.3575-15.2016>
- Wilkinson-Berka, J. L., Wraight, C., & Werther, G. (2006). The role of growth hormone, insulin-like growth factor and somatostatin in diabetic retinopathy. *Current Medicinal Chemistry*, 13(27), 3307–3317. <https://doi.org/10.2174/092986706778773086>
- Witmer, A. N., Vrensen, G. F., Van Noorden, C. J., & Schlingemann, R. O. (2003). Vascular endothelial growth factors and angiogenesis in eye disease. *Progress in Retinal and Eye Research*, 22(1), 1–29. [https://doi.org/10.1016/s1350-9462\(02\)00043-5](https://doi.org/10.1016/s1350-9462(02)00043-5)
- Wrana, J. L., Attisano, L., Wieser, R., Ventura, F., & Massague, J. (1994). Mechanism of activation of the TGF-beta receptor. *Nature*, 370(6488), 341–347. <https://doi.org/10.1038/370341a0>
- Writing Committee for the Diabetic Retinopathy Clinical Research, Gross, J. G., Glassman, A. R., Jampol, L. M., Inusah, S., Aiello, L. P., ... Beck, R. W. (2015). Panretinal photocoagulation vs Intravitreal Ranibizumab for proliferative diabetic retinopathy: A randomized clinical trial. *JAMA*, 314(20), 2137–2146. <https://doi.org/10.1001/jama.2015.15217>
- Xiao, S., Bucher, F., Wu, Y., Rokem, A., Lee, C. S., Marra, K. V., ... Lee, A. Y. (2017). Fully automated, deep learning segmentation of oxygen-induced retinopathy images. *JCI Insight*, 2(24), e97585. <https://doi.org/10.1172/jci.insight.97585>
- Yamashita, H., ten Dijke, P., Franzen, P., Miyazono, K., & Heldin, C. H. (1994). Formation of hetero-oligomeric complexes of type I and type II receptors for transforming growth factor-beta. *The Journal of Biological Chemistry*, 269(31), 20172–20178. <https://www.ncbi.nlm.nih.gov/pubmed/8051105>
- Yin, J., Xu, W. Q., Ye, M. X., Zhang, Y., Wang, H. Y., Zhang, J., ... Wang, Y. S. (2017). Up-regulated basigin-2 in microglia induced by hypoxia promotes retinal angiogenesis. *Journal of Cellular and Molecular Medicine*, 21(12), 3467–3480. <https://doi.org/10.1111/jcmm.13256>
- Zhao, L., Zabel, M. K., Wang, X., Ma, W., Shah, P., Fariss, R. N., ... Wong, W. T. (2015). Microglial phagocytosis of living photoreceptors contributes to inherited retinal degeneration. *EMBO Molecular Medicine*, 7(9), 1179–1197. <https://doi.org/10.15252/emmm.201505298>
- Zoller, T., Schneider, A., Kleimeyer, C., Masuda, T., Potru, P. S., Pfeifer, D., ... Spittau, B. (2018). Silencing of TGFbeta signalling in microglia results in impaired homeostasis. *Nature Communications*, 9(1), 4011. <https://doi.org/10.1038/s41467-018-06224-y>

#### SUPPORTING INFORMATION

Additional supporting information may be found in the online version of the article at the publisher's website.

**How to cite this article:** Usui-Ouchi, A., Eade, K., Giles, S., Ideguchi, Y., Ouchi, Y., Aguilar, E., Wei, G., Marra, K. V., Berlow, R. B., & Friedlander, M. (2022). Deletion of Tgfb signal in activated microglia prolongs hypoxia-induced retinal neovascularization enhancing Igf1 expression and retinal leukostasis. *Glia*, 70(9), 1762–1776. <https://doi.org/10.1002/glia.24218>